Geophysical Research Letters

RESEARCH LETTER
10.1029/2024GL108728

Emergent Constraints on Future Projections of Tibetan Plateau Warming in Winter

Shuzhen Hu[1], Lu Wang[1,2], Xiaolong Chen[3], Tianjun Zhou[3,4], and Pang-Chi Hsu[1]

[1]Key Laboratory of Meteorological Disaster, Ministry of Education (KLME)/Collaborative Innovation Center on Forecast and Evaluation of Meteorological Disasters (CIC-FEMD), Nanjing University of Information Science and Technology, Nanjing, China, [2]Laboratory for Regional Oceanography and Numerical Modeling, Qingdao National Laboratory for Marine Science and Technology, Qingdao, China, [3]State Key Laboratory of Numerical Modeling for Atmospheric Sciences and Geophysical Fluid Dynamics, Institute of Atmospheric Physics, Chinese Academy of Sciences, Beijing, China, [4]College of Earth and Planetary Sciences, The University of Chinese Academy of Sciences, Beijing, China

Abstract The Tibetan Plateau (TP) is an area highly sensitive to climate change and is warming faster than the global average. The TP temperature change has a significant impact on the local ecological environment and the downstream weather and climate. The TP will undoubtedly warm in the future, but the warming extent is uncertain. Using the Coupled Model Inter-comparison Project Phase 6 multi-model ensemble, we found that models simulating smaller TP temperature increases in recent decades tend to project weaker warming in the future. This relationship is driven by the simulation of snowmelt response to greenhouse gas increases, as snow-related albedo feedback dominates the TP temperature changes in both historical and future periods. Based on a two-step emergent constraint approach, the rectified TP warming magnitude increases by about 0.3°C compared to the unconstrained result under both the medium and high emission scenarios, and the inter-model uncertainty is reduced by about 60%.

Plain Language Summary The Tibetan Plateau (TP), known as "the third pole of the world," is the highest terrain on Earth. It has experienced a rapid increase in surface temperature over the past few decades, which has significantly impacted the local ecological environment and downstream weather and climate. Therefore, how the surface temperature of the TP will change in the future is of concern to both the scientific community and society at large. Although a future warming trend over the TP is evident in model projections, the extent of this warming remains highly uncertain. Based on a multi-model ensemble, we found that the projected temperature change over the TP during the boreal winter is significantly influenced by the simulation of TP temperature changes in recent decades, which is related to model sensitivities in simulating the snowmelt rate in response to greenhouse gas increases. Removing the model bias using observations would further increase the projected future warming over the TP, meaning that humanity will face greater challenges.

Key Points:

- A two-step emergent constraint (EC) technique is developed for projections of the Tibetan Plateau (TP) warming in the boreal winter
- The EC arises from model sensitivities in simulating snow cover change in response to greenhouse gas increases
- Constrained results effectively reduce inter-model uncertainty and show stronger warming over the TP than the original results

Supporting Information:

Supporting Information may be found in the online version of this article.

Correspondence to:

L. Wang and P.-C. Hsu,
luwang@nuist.edu.cn;
pangchi@nuist.edu.cn

Citation:

Hu, S., Wang, L., Chen, X., Zhou, T., & Hsu, P.-C. (2024). Emergent constraints on future projections of Tibetan Plateau warming in winter. *Geophysical Research Letters*, *51*, e2024GL108728. https://doi.org/10.1029/2024GL108728

Received 6 SEP 2023
Accepted 16 APR 2024

Author Contributions:

Conceptualization: Lu Wang
Formal analysis: Shuzhen Hu
Funding acquisition: Lu Wang
Investigation: Shuzhen Hu
Supervision: Lu Wang
Writing – original draft: Shuzhen Hu, Lu Wang
Writing – review & editing: Lu Wang, Xiaolong Chen, Tianjun Zhou, Pang-Chi Hsu

1. Introduction

The Tibetan Plateau (TP), the highest terrain on Earth, is known as "the third pole of the world" (Qiu, 2008). In recent decades, the TP has experienced rapid warming due to the anthropogenic greenhouse effect, especially during boreal winter (A. Duan & Xiao, 2015; You et al., 2017; T. Zhou & Zhang, 2021). The warming rate over the TP area in winter is about 1.84 times the global average from 1979 to 2020 (S. Hu et al., 2023), referred to as TP warming amplification (J. Duan et al., 2020; Wang et al., 2014; You et al., 2020). This severe TP warming has already caused adverse impacts such as melting permafrost, retreating glaciers, and declining biodiversity (M. Yang et al., 2019; Yao et al., 2019; You, Cai, Pepin, et al., 2021). The rapid warming of this region and its potential magnitude in the future are of great concern to both society and the scientific community.

Climate models are widely used to study the future projections of climate change (e.g., Beniston et al., 2007; X. Chen & Zhou, 2016; Sharmila et al., 2015). All models project that the TP surface temperature will continue to increase under future warming climate (e.g., Fan et al., 2022; Guo et al., 2016; F. Su et al., 2013), but consensus on its future warming magnitude remains lacking. The magnitude of temperature increase could be influenced by emission scenarios (Tian et al., 2015; You, Cai, Wu, et al., 2021; M. Zhou et al., 2022), with the projected difference between the very high and very low emission scenarios reaching as much as 6°C by the end of the 21st century (Y. Peng et al., 2022). Furthermore, the projected TP temperature increase shows significant inter-model variation even under the same scenario, owing to model discrepancies in their dynamical framework,

parameterization, and coupling schemes, etc. (e.g., Hodson et al., 2013; Hojberg & Refsgaard, 2005; Refsgaard et al., 2006). Such uncertainties cast doubt on the credibility of the projected TP temperature changes from the default models.

Given that accurate projection of the magnitude of TP warming is essential for effective policy making and adaptation to climate change, previous efforts have attempted to examine the inter-model variation in temperature changes over the TP in order to constrain the projections. A recent paper by Y. Peng et al. (2022) attempted to rectify the winter surface air temperature change over the TP, based on the statistical downscaling method for selected optimal models. Their results suggested that, under the SSP5-8.5 high emissions scenario, the adjusted TP-averaged warming by the end of the 21st century is 0.06°C higher than expected by the ensemble average of the 32 Coupled Model Intercomparison Project Phase 6 (CMIP6) models. While this study provided valuable information, whether the results would be sensitive to different methods remains unclear. The emergent constraint (EC) method, based on a tight linkage between the inter-model spread in an observable predictor and climate projection (Allen & Ingram, 2002; Brient, 2020), has demonstrated robust capability in reducing the uncertainty in projecting Earth system variables simulated by a multi-model ensemble (MME) and has been widely applied to constrain climate change to achieve more reliable climate projections (e.g., Cox et al., 2018; Hall & Qu, 2006; Shiogama et al., 2022; Yu et al., 2022). However, we are not aware of any specific application of this method to constrain the future change in surface air temperature over the TP in the CMIP6 models. Hence, this method will be applied in this study to constrain the future warming of the TP.

Several physical processes are involved in the surface air temperature change, including surface albedo feedback, water vapor feedback, cloud feedback, radiative forcing, Planck feedback, lapse rate feedback, surface heat flux (SHF), and atmospheric heat transport (AHT) (Gao et al., 2019; Goosse et al., 2018). Many efforts have been made to identify the dominant physical processes responsible for the observed and the projected warming trend of the TP temperature (e.g., A. Duan & Wu, 2006; Liu et al., 2009; Rangwala et al., 2009; J. Zhang et al., 2022). For instance, a recent paper (S. Hu et al., 2023) quantified the relative effects of eight physical processes on TP warming and suggested that snow-albedo feedback is not only the leading contributor to TP warming in recent decades but also in the late 21st century. However, it is important to note that previous studies have primarily focused on MME averages and have yet to identify the main physical processes that account for inter-model variation in TP temperature change. Understanding the relationship between future climate change and historical simulations is crucial in developing an EC approach suitable for the warming of the TP, and revealing the key physical processes responsible for the inter-model variation of the TP temperature projection can aid in this understanding.

In this study, we aim to answer the following questions: (a) What is the dominant physical process that leads to the inter-model spread of projected winter surface temperature change over the TP in CMIP6 models? (b) Can we use the identified physical process to develop an EC method that effectively reduces the uncertainty in the projection of TP temperature change?

2. Data and Methods

2.1. Simulated and Observational Data

Historical simulations and future projections under the SSP2-4.5 and SSP5-8.5 scenarios (O'Neill et al., 2016) of 28 CMIP6 models (Table S1 in Supporting Information S1) were used, so that the TP warming at a medium and a high level of greenhouse gas emission can be compared. The model selection was based on the availability of the 19 variables (Table S2 in Supporting Information S1) required for the local energy budget diagnosis, which is used to reveal the key physical process responsible for the projection uncertainty of the TP warming. Only one ensemble member (r1i1p1f1) from each model was analyzed.

The 2-m air temperature (T_{2m}) from the China meteorological forcing data set (CMFD, He et al., 2020) and the National Climate Center of China Meteorological Administration data set (CN05.1, J. Wu & Gao, 2013) are selected as the observational data for calibrating future projections. This is because these two data sets have the best quality among 10 commonly used gridded air temperature products and are in good agreement with real ground-site observations (X. Peng et al., 2021; J. Wu et al., 2017).

2.2. Quantifications of Processes Causing the TP Temperature Change

Several budget diagnosis methods can be used to quantify the relative effects of different physical processes on T_{2m} change over the TP (Lu & Cai, 2009; Soden et al., 2008), such as the surface energy balance analysis (e.g., Gao et al., 2019; J. Su et al., 2017) and the coupled surface-air feedback response analysis method (e.g., X. Hu et al., 2017; Y. Wu et al., 2020). However, the former cannot explicitly show the physical processes associated with the Planck feedback, lapse rate feedback, water vapor feedback, and AHT that are important for temperature change, and the latter cannot resolve the contribution of the temperature feedback. To avoid the above problems, we used the local energy budget diagnosis, considering all eight physical processes to quantify their contribution to surface temperature changes on the TP. This approach has been applied to understand the polar amplification (e.g., Goosse et al., 2018; Pithan & Mauritsen, 2014) and the TP warming (e.g., Hu & Hsu, 2023; R. Zhang et al., 2020). The budget equation can be written as (Goosse et al., 2018):

$$\Delta T_{2m} = -\underbrace{\frac{F}{\overline{\lambda_0}}}_{CO_2} - \underbrace{\frac{\lambda_0 \Delta T_{2m}}{\overline{\lambda_0}}}_{P'} - \underbrace{\frac{\lambda_1 \Delta T_{2m}}{\overline{\lambda_0}}}_{\text{LR}} - \underbrace{\frac{\lambda_2 \Delta T_{2m}}{\overline{\lambda_0}}}_{\text{Albedo}} - \underbrace{\frac{\lambda_3 \Delta T_{2m}}{\overline{\lambda_0}}}_{\text{WV}} - \underbrace{\frac{\lambda_4 \Delta T_{2m}}{\overline{\lambda_0}}}_{\text{Cloud}} - \underbrace{\frac{\Delta \text{SHF}}{\overline{\lambda_0}}}_{\text{SHF}} - \underbrace{\frac{\Delta \text{AHT}}{\overline{\lambda_0}}}_{\text{AHT}}, \quad (1)$$

where Δ denotes the future change, which refers to the difference in winter (December–February) climatology between the periods of 2071–2100 and 1985–2014. The terms on the right-hand side of Equation 1 represent in turn T_{2m} changes induced directly by radiative forcing (CO_2), Planck feedback (P'), lapse rate feedback (LR), surface albedo feedback (Albedo), water vapor feedback (WV), cloud feedback (Cloud), SHF, and AHT, respectively. λ_i denote feedback parameters, which are calculated by the radiative kernel method developed by Soden et al. (2008) (Text S1 in Supporting Information S1).

2.3. Statistical Framework of Emergent Constraint

The EC approach utilizes the MME to identify a significant linear relationship between an uncertain aspect of the future climate (referred to as predictand or Y) and an observable variable in the contemporary climate (referred to as predictor or X). The observations of X (referred to as X_O) are used to calibrate Y with the following equations (Bowman et al., 2018; X. Chen et al., 2020):

$$\overline{Y_C} = \overline{Y} + \frac{r}{1 + \text{SNR}^{-1}}\left(\overline{X_O} - \overline{X}\right), \quad (2)$$

$$\sigma^2_{Y_C} = \left(1 - \frac{\rho^2}{1 + \text{SNR}^{-1}}\right)\sigma^2_Y, \quad (3)$$

$$\text{TRV} = \frac{\rho^2}{1 + \text{SNR}^{-1}} \times 100\%, \quad (4)$$

where Y_C represents the constrained results of Y, σ^2 represents variance, and TRV represents totally reduced model variance. r and ρ are the regression coefficient and correlation coefficient between Y and X, respectively. An overbar denotes expectation, and SNR is the signal-to-noise ratio calculated by comparing the variance of X across models to that of X_O across different observational data sets.

3. Results

3.1. Key Processes Causing the Inter-Model Spread of Future TP Warming

The temporal evolution of T_{2m} changes over the TP exhibits a wide range among the CMIP6 models (Figure 1a), with the year 2100 showing the largest inter-model difference of 5.74°C (7.51°C) under the SSP2-4.5 (SSP5-8.5) scenario. This uncertainty range is even greater than the MME mean result of 3.39°C (7.00°C). To understand this wide range of warming magnitude, we decomposed the future TP temperature change into components induced by different physical processes (Equation 1). In terms of the MME mean results (middle line of each box in Figure 1b), the Albedo process plays the leading role, increasing the TP temperature by 1.16°C (2.24°C) under the SSP2-4.5 (SSP5-8.5) scenario and accounting for 39% of the MME mean warming magnitude. This is twice as

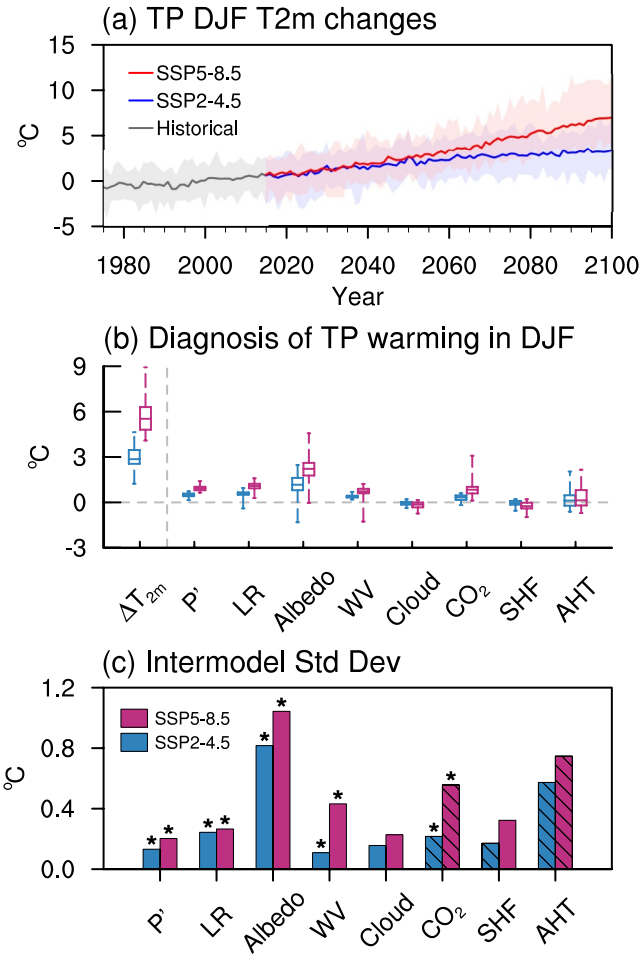

Figure 1. (a) Temporal evolutions of winter T_{2m} changes (units: °C) over the Tibetan Plateau (TP) relative to the average of 1985–2014. The gray, blue, and red lines (shadings) denote the multi-model ensemble mean (ensemble spread) of 28 Coupled Model Intercomparison Project Phase 6 models under the Historical, SSP2-4.5, and SSP5-8.5 simulations, respectively. The ensemble spread is estimated by the difference between the maximum and the minimum results among models. (b) ΔT_{2m} and the relative contributions of eight physical processes (see Equation 1) under the SSP2-4.5 (blue) and SSP5-8.5 (magenta) scenarios, respectively. The values presented in the box plots are the minimum (lower bound), the 25th percentile (lower quartile), the median (central line), the 75th percentile (upper quartile), and the maximum (upper bound) of the analyzed models. (c) The inter-model standard deviation (units: °C) of ΔT_{2m} induced by each physical process under the SSP2-4.5 (blue bars) and SSP5-8.5 (red bars) scenarios, respectively. The bars with (without) diagonal slashes denote that the inter-model correlation between ΔT_{2m} and that induced by each physical process is negative (positive), and the correlation coefficients significant at the 95% confidence level based on the Student's *t*-test are marked by asterisks. The diagnostic results in panels (b, c) were based on the TP temperature changes between 2071–2100 and 1985–2014.

large as the LR, which is the secondary contributor and increases the TP temperature by 0.57°C (1.09°C) under the SSP2-4.5 (SSP5-8.5) scenario. When focusing on the inter-model spread, the Albedo and AHT processes show the largest inter-model variances (whiskers in Figure 1b and bars in Figure 1c). However, the inter-model correlation between ΔT_{2m} and these two physical processes shows opposite results. The projected Albedo (AHT) shows a positive (negative) correlation coefficient (Figure 1c), indicating a positive (negative) contribution to the inter-model spread of TP warming. Therefore, we argue that the projected Albedo process is the dominant contributor to the large inter-model spread of future TP warming, and the latter could be constrained to a large extent after constraining the projected result of Albedo.

3.2. Two-Step Constraint on TP Warming Magnitude

Here, we develop a two-step method to constrain the magnitude of projected TP warming, which first applies EC to the projected Albedo, and then rectifies the future TP warming based on the constrained result derived from the first step. The adoption of this two-step analysis is because its derivation is physically based and it has a better result in reducing the inter-model uncertainty than the common one-step approach, which directly applies EC to the projected TP warming (figures not shown).

First, we sought to identify an appropriate predictor for projected Albedo. Previous studies have used the temperature trend during an arbitrarily selected historical period to constrain future temperature change (e.g., Z. Chen et al., 2023), without considering the unstable nature of climate systems. A very recent study (Shen et al., 2023), however, proposed to select an optimal historical period for calibration, taking into account the potential effect of time-varying climate over different historical periods, so that a more reasonable constrained result could be obtained. To select an objective and optimal historical period for the predictor, we calculated the inter-model correlation between the simulated TP temperature changes over different historical periods relative to a fixed climatology (1985–2014) and the projected changes in Albedo (2071–2100) (Figures S1b and S1c in Supporting Information S1). The correlation relationship appears to vary with time and is only robust when the calculation is based on recent years. The TP temperature change over 1997–2018 shows the highest correlation coefficient with the future changes in Albedo (marked by stars). This indicates the unstable nature of the TP climate, and the TP temperature change at the end of the 21st century is more closely related to the change in recent decades than in earlier decades. In fact, the TP warming rate has become faster in recent decades than in earlier decades (Figure S1a in Supporting Information S1).

The significant inter-model correlation between the historical and future temperature changes over the TP can be explained by the simulation of snow cover, as snow-related albedo feedback dominates the TP temperature changes in both historical (S. Hu et al., 2023) and future periods (Figure 1b). In the current climate, the models that simulate a faster snowmelt rate tend to simulate a larger increase in TP temperature during the historical period (Figures 2a and 2b), with an inter-model correlation of −0.59 (−0.72) under SSP2-4.5 (SSP5-8.5). This is because a decrease in snow cover can reduce the surface albedo, which in turn leads to more incident solar radiation. Such a difference in model sensitivity of snowmelt response over the TP found in the historical period will also exist in the future climate, with a correlation between the two quantities of 0.77 (0.8) under SSP2-4.5 (SSP5-8.5) (Figures 2c and 2d). The latter further leads to an inter-model discrepancy in the projections of surface albedo over the TP (Figures 2e and 2f), and thus induces different magnitudes of future TP

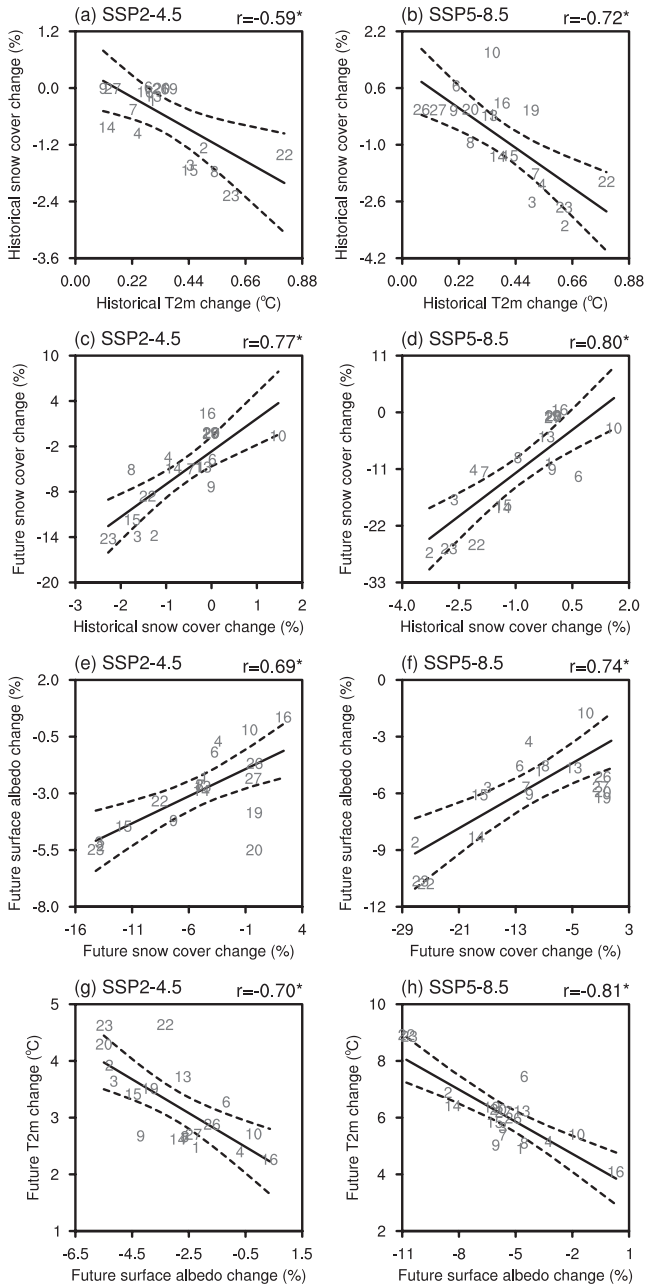

Figure 2. Inter-model relationship between (a, b) the changes in temperature and snow cover during historical period, (c, d) changes in snow cover during historical and future periods, (e, f) changes in snow cover and surface albedo during future period, and (g, h) changes in surface albedo and temperature during future period. The historical (future) change is calculated from 1997–2018 (2071–2100) minus 1985–2014. The results are all based on Tibetan Plateau-averaged results in winter. The left (right) panels are under the SSP2-4.5 (SSP5-8.5) scenario. The numbers correspond to each of the analyzed models (see the information in Table S1 in Supporting Information S1). The inter-model correlation coefficients are shown on the upper right corner of each panel and those significant at the 95% confidence level are marked by asterisks. The solid fitting line is obtained by the least square method and dashed curves denote the 95% confidence range of the linear regression.

warming (Figures 2g and 2h) through the surface-albedo feedback process, all of which show a significant inter-model correlation relationship.

The physically supported and statistically significant relationship between historical and future temperature changes provides an EC on the projected magnitude of TP warming. Figure 3 presents the results corresponding to our two-step analysis. In the first step, the present-day TP temperature change in recent decades (1997–2018) is used as a predictor of the projected Albedo (2071–2100), where the correlation coefficient between these two quantities is 0.52 for SSP2-4.5 and 0.49 for SSP5-8.5, respectively, both significant at the 95% confidence level (Figures 3a and 3b). Based on the hierarchical statistical framework (Equations 2 and 3), the constrained Albedo increases by 0.35 (0.31)°C under SSP2-4.5 (SSP5-8.5), and the uncertainty range decreases by 23% (21%). Next, the constrained Albedo change (vertical dashed lines in Figures 3c and 3d) is used to correct the TP total warming, as the two quantities are highly correlated with a coefficient of nearly 0.8. Figures 3e and 3f compare the probability density functions of the constrained and unconstrained total TP warming in the future. The uncertainty of the projections decreases by 59% (60%) under the SSP2-4.5 (SSP5-8.5) scenario, and the MME mean of the total TP temperature change increases by approximately 0.25°C (0.28°C) compared to the original result.

Two approaches were used to verify the authenticity of the constrained results. First, we evaluated the observationally constrained TP temperature changes for the historical period. Since the future simulations of the models start from 2015, the validation period was chosen as 2015–2022. We used the relationship between observations and historical simulations (2002–2013) to constrain the simulated temperature in 2015–2022. The selection of the best historical period to constrain follows the same analysis procedure as shown in Section 3.2 (figures not shown). The difference between the constrained results and the actual observation during the validation period is significantly reduced compared to that for the unconstrained results (Figure S2 in Supporting Information S1), as the root-mean-square error of the biases is reduced from 0.64 to 0.09 (from 0.70 to 0.36) for the SSP2-4.5 (SSP5-8.5) results. Second, we applied a leave-one-out perfect model test for the projection period (Text S2 in Supporting Information S1). As shown in Figure 4, most of the constrained projections align more closely with the pseudo-warming than the unconstrained projections, with only ~18% out of all the 28 models falling completely outside the 5th–95th confidence range of the constrained projections under SSP5-8.5. Furthermore, the constrained projections show lower values for the two statistics, namely mean square error and continuous ranked probability skill score, compared to the unconstrained projections. This indicates that the constrained projections are of high quality. Overall, the results from both methods demonstrate the validity of the constrained results obtained from our two-step EC method.

4. Conclusions

How the observed warming over the TP will continue in the future is of great concern to both the scientific community and policy makers. However, existing projections show large uncertainties in their magnitude. Here, based on the outputs of 28 CMIP6 models under both the medium (SSP2-4.5) and the high (SSP5-8.5) emission scenarios, we have developed a two-step EC approach and effectively reduced the uncertainty in the projections of future TP warming in the boreal winter.

10.1029/2024GL108728

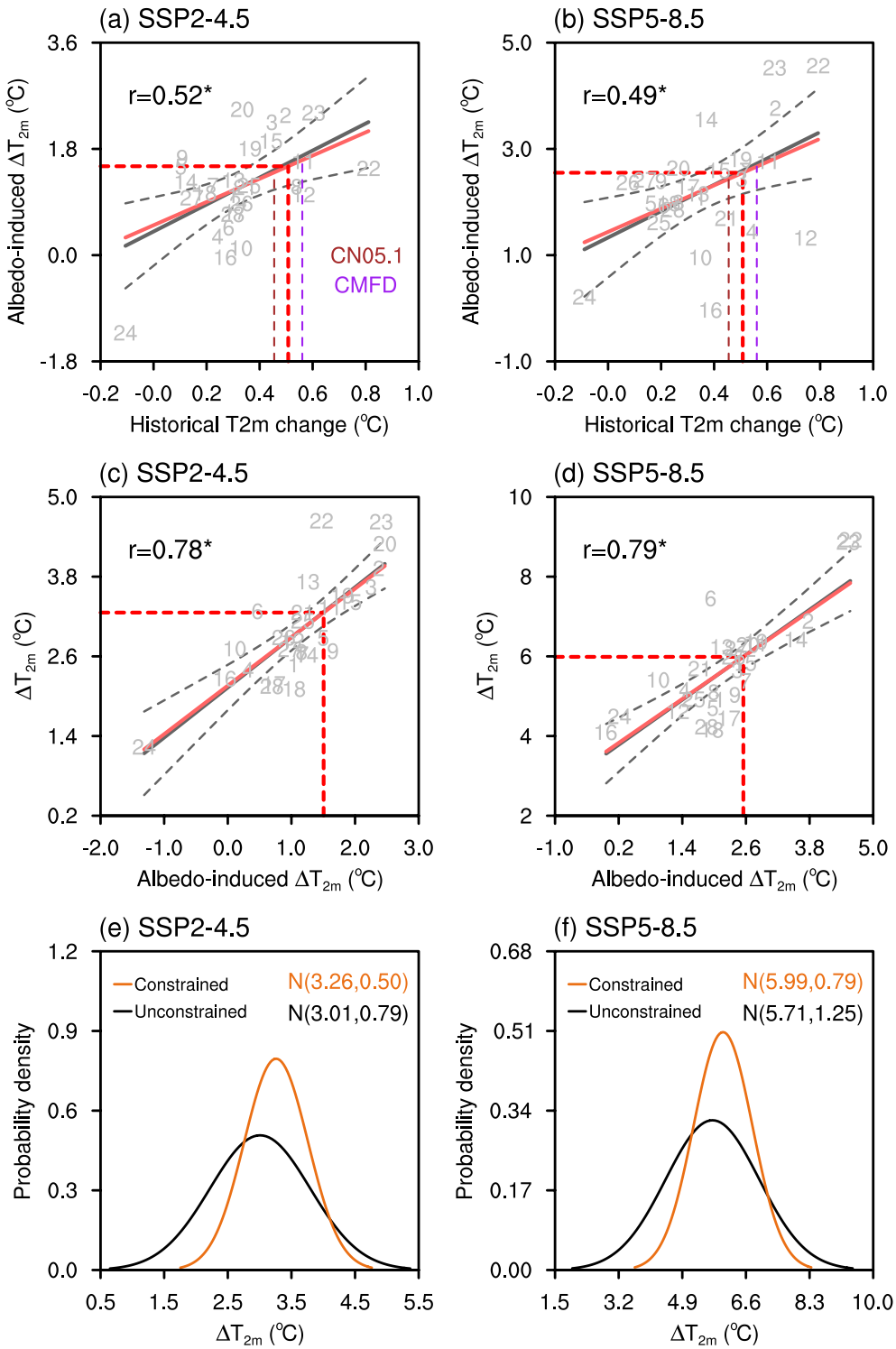

Figure 3. (a, b) As in Figure 2, but for inter-model relationship between (a, b) historical temperature change and future Albedo-induced temperature change, and (c, d) future changes in Albedo-induced temperature and total temperature. Brown and purple vertical dashed lines represent the observational results derived from CN05.1 and CMFD, respectively, and their mean is represented by the red vertical dashed lines. Red solid fitting lines represent observational corrections based on Equation 2, while red horizontal dashed lines are the constrained result based on historical Tibetan Plateau (TP) temperature change. (e, f) Probability density function based on the Gaussian assumption of unconstrained (black) and constrained (orange) results of future change in T_{2m} over the TP under the SSP2-4.5 and SSP5-8.5, respectively.

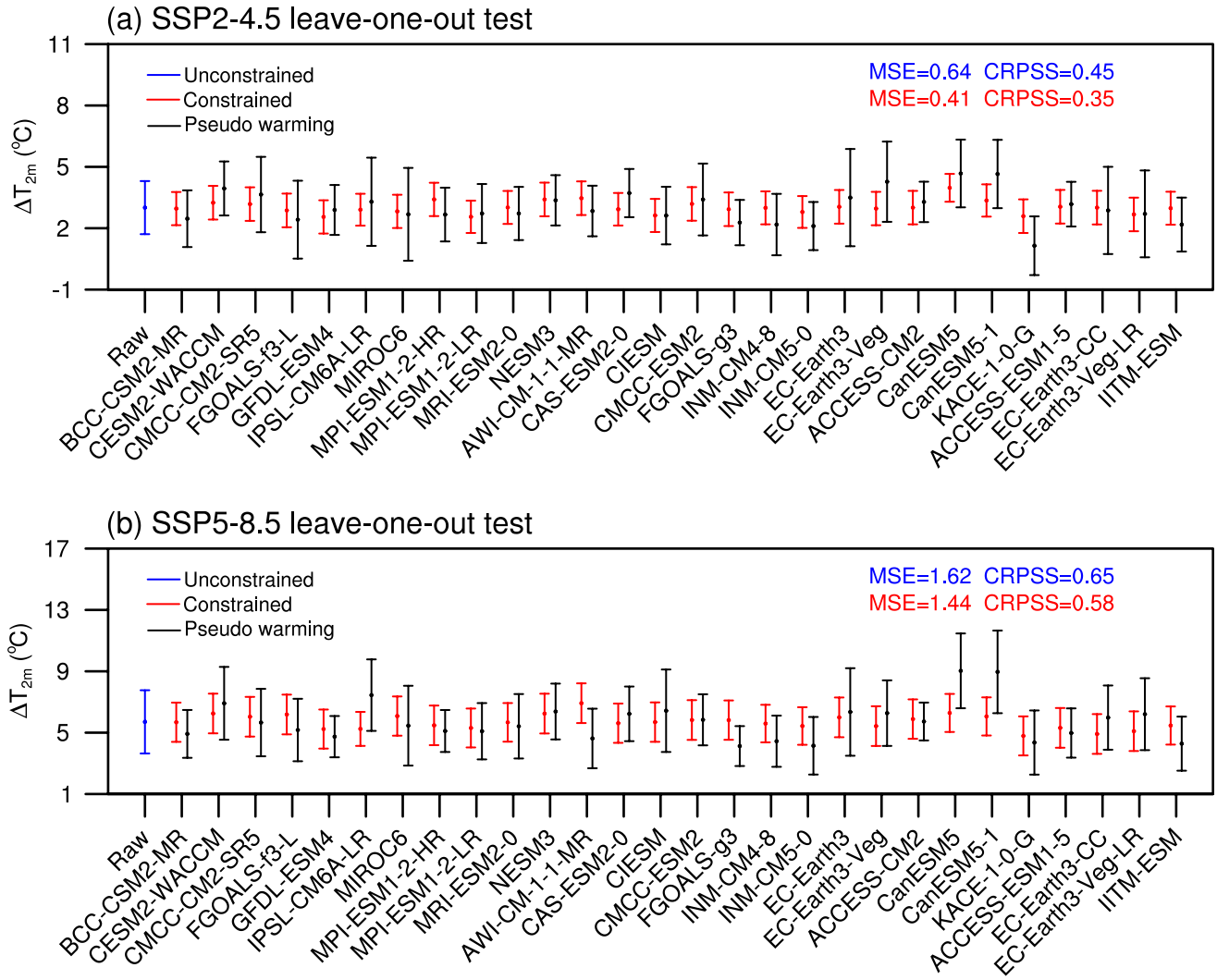

Figure 4. The leave-one-out perfect model test for the future Tibetan Plateau (TP) warming under the (a) SSP2-4.5 and (b) SSP5-8.5 scenarios, respectively. We remove the projected warming of the targeted model and set it as the pseudo warming (black) and then constrain the projected warming of the remaining models by the present-day TP temperature change using our two-step approach (Text S2 in Supporting Information S1). The constrained (unconstrained) projections are displayed in red (blue), with the corresponding mean square error and continuous ranked probability skill score values given in the upper-right corner of each panel. The dots indicate the multi-model ensemble means, while the vertical lines denote the range of the 5th and 95th percentiles. For the target model, the range is represented by the spread of the 5th and 95th percentiles of future TP warming for 2071–2100.

We found that the projected temperature changes over the TP (2071–2100) are significantly influenced by their changes in recent decades (1997–2018), with models simulating smaller (larger) temperature increases in the contemporary climate projecting weaker (stronger) Albedo process in the future. The latter is the dominant contributor to the inter-model spread in projections of TP warming, as revealed by the local energy budget diagnostics (Equation 1). The significant historical-future relationship arises from model sensitivities in simulating the snowmelt rate in response to greenhouse gas increases, which are highly consistent from history to the future. A more rapid decline in snow cover in the historical (future) period would result in a correspondingly greater increase in temperature over the TP. The projected Albedo process is constrained by historical TP temperature change, and the obtained result is then used to rectify the projected total temperature change over the TP. The constrained results reduce about 60% of the inter-model spread in the future projections compared to the unconstrained ones, and the MME mean warming magnitude averaged for 2071–2100 increases by about 0.3°C, reaching 3.3°C (6.0°C) under the SSP2-4.5 (SSP5-8.5) scenarios. The increased warming magnitude after the correction suggests a more severe situation for local ecosystems over the TP, which are already suffering from warming threats.

The innovation of this work is that it first reveals the key physical processes that cause the inter-model uncertainty in projections of TP temperature change, which facilitates the identification of an appropriate observational constraint and the interpretation of the future-historical relationship. We have also calculated the results by applying the EC directly to the future change in total temperature over the TP, and the results show a reduction in inter-model uncertainty of about 18% under the SSP5-8.5 scenarios (figures not shown), which is less than our results. This further demonstrates the advantage of the two-step EC technique developed in this study over the conventionally used one-step approach. Note that the analysis process of this study is based on regional average results. To verify its authenticity, we further examined the horizontal distribution of the inter-model relationship of some critical results. Figure S3 in Supporting Information S1 presents the correlation between the total temperature change and that induced by Albedo, as well as the correlation between the Albedo-induced future temperature change and the TP temperature change in the historical period. Most regions of the TP exhibit significant positive correlations, which supports our findings based on the TP-domain averages (refer to Figures 1c, 3a, and 3b). However, there are still some regional inhomogeneities in the distribution of correlation coefficients, which may be due to the complex topography of the TP. This suggests the need to consider the effect of the TP topography in future constraint studies.

Data Availability Statement

The Historical simulations, the SSP2-4.5 scenario simulates and the SSP5-8.5 scenario simulates outputs used in this study can be obtained from the CMIP6 archives at https://esgf-node.llnl.gov/search/cmip6/. The CMIP6 models used in the study are listed in Table S1 in Supporting Information S1. The CMFD data can be obtained from K. Yang et al. (2019). The observational data CN05.1 can be obtained from S. Hu (2023b). The RRTM_ERAI radiative kernels, CAM3 radiative kernels, HadGEM3-GA7.1 radiative kernels, and CESM-CAM5 radiative kernels can be obtained from Huang (2022), S. Hu (2023a), Smith (2019), and Pendergrass (2017), respectively. The CloudSat radiative kernels can be obtained from https://climate.rsmas.miami.edu/data/radiative-kernels/.

Acknowledgments
The work is supported by the National Key Research and Development Program of China (Grant 2020YFA0608901) and the National Natural Science Foundation of China (Grants 41988101 and 42088101). We acknowledge the High Performance Computing Center of Nanjing University of Information Science & Technology for their support of this work.

References

Allen, M. R., & Ingram, W. J. (2002). Constraints on future changes in climate and the hydrologic cycle. *Nature*, *419*(6903), 224–232. https://doi.org/10.1038/nature01092

Beniston, M., Stephenson, D. B., Christensen, O. B., Ferro, C. A. T., Frei, C., Goyette, S., et al. (2007). Future extreme events in European climate: An exploration of regional climate model projections. *Climatic Change*, *81*(1), 71–95. https://doi.org/10.1007/s10584-006-9226-z

Bowman, K. W., Cressie, N., Qu, X., & Hall, A. (2018). A hierarchical statistical framework for emergent constraints: Application to snow albedo feedback. *Geophysical Research Letters*, *45*(23), 13050–13059. https://doi.org/10.1029/2018GL080082

Brient, F. (2020). Reducing uncertainties in climate projections with emergent constraints: Concepts, examples and prospects. *Advances in Atmospheric Sciences*, *37*, 1–15. https://doi.org/10.1007/s00376-019-9140-8

Chen, X., & Zhou, T. (2016). Uncertainty in crossing time of 2°C warming threshold over China. *Science Bulletin*, *61*(18), 1451–1459. https://doi.org/10.1007/s11434-016-1166-z

Chen, X., Zhou, T., Wu, P., Guo, Z., & Wang, M. (2020). Emergent constraints on future projections of the western North Pacific subtropical high. *Nature Communications*, *11*(1), 2802. https://doi.org/10.1038/s41467-020-16631-9

Chen, Z., Zhou, T., Chen, X., Zhang, W., Zuo, M., Man, W., & Qian, Y. (2023). Emergent constrained projections of mean and extreme warming in China. *Geophysical Research Letters*, *50*(20), e2022GL102124. https://doi.org/10.1029/2022GL102124

Cox, P., Huntingford, C., & Williamson, M. (2018). Emergent constraint on equilibrium climate sensitivity from global temperature variability. *Nature*, *553*(7688), 319–322. https://doi.org/10.1038/nature25450

Duan, A., & Wu, G. (2006). Change of cloud amount and the climate warming on the Tibetan Plateau. *Geophysical Research Letters*, *33*(22), L22704. https://doi.org/10.1029/2006GL027946

Duan, A., & Xiao, Z. (2015). Does the climate warming hiatus exist over the Tibetan Plateau? *Scientific Reports*, *5*(1), 13711. https://doi.org/10.1038/srep13711

Duan, J., Li, L., Chen, L., & Zhang, H. (2020). Time-dependent warming amplification over the Tibetan Plateau during the past few decades. *Atmospheric Science Letters*, *21*(10), e998. https://doi.org/10.1002/asl.998

Fan, X., Duan, Q., Shen, C., Wu, Y., & Xing, C. (2022). Evaluation of historical CMIP6 model simulations and future projections of temperature over the pan-third pole region. *Environmental Science and Pollution Research*, *29*(18), 26214–26229. https://doi.org/10.1007/s11356-021-17474-7

Gao, K., Guan, A., Chen, D., & Wu, G. (2019). Surface energy budget diagnosis reveals possible mechanism for the different warming rate among the three poles on Earth in recent decades. *Science Bulletin*, *64*(16), 1140–1143. https://doi.org/10.1016/j.scib.2019.06.023

Goosse, H., Kay, J. E., Armour, K. C., Bodas-Salcedo, A., Chepfer, H., Docquier, D., et al. (2018). Quantifying climate feedbacks in polar regions. *Nature Communications*, *9*(1), 1919. https://doi.org/10.1038/s41467-018-04173-0

Guo, D., Yu, E., & Wang, H. (2016). Will the Tibetan Plateau warming depend on elevation in the future. *Journal of Geophysical Research: Atmospheres*, *121*(8), 3969–3978. https://doi.org/10.1002/2016JD024871

Hall, A., & Qu, X. (2006). Using the current seasonal cycle to constrain snow albedo feedback in future climate change. *Geophysical Research Letters*, *33*(3), L03502. https://doi.org/10.1029/2005GL025127

He, J., Yang, K., Tang, W., Lu, H., Qin, J., Chen, Y., & Li, X. (2020). The first high-resolution meteorological forcing dataset for land process studies over China. *Scientific Data*, *7*(1), 25. https://doi.org/10.1038/s41597-020-0369-y
Hodson, D. L. R., Keeley, S. P. E., West, A., Ridley, J., Hawkins, E., & Hewitt, H. T. (2013). Identifying uncertainties in Arctic climate change projections. *Climate Dynamics*, *40*(11–12), 2849–2865. https://doi.org/10.1007/s00382-012-1512-z
Hojberg, A. L., & Refsgaard, J. C. (2005). Model uncertainty-parameter uncertainty versus conceptual models. *Water Science and Technology*, *52*(6), 177–186. https://doi.org/10.2166/wst.2005.0166
Hu, S. (2023a). CAM3 radiative kernel [Dataset]. *Zenodo*. https://doi.org/10.5281/zenodo.8320575
Hu, S. (2023b). CN05.1 [Dataset]. *Zenodo*. https://doi.org/10.5281/zenodo.8320581
Hu, S., & Hsu, P.-C. (2023). Drivers of elevation-dependent warming over the Tibetan Plateau. *Atmospheric and Oceanic Science Letters*, *16*(2), 100289. https://doi.org/10.1016/j.aosl.2022.100289
Hu, S., Hsu, P.-C., Li, W., Wang, L., Chen, H., & Zhou, B. (2023). Mechanisms of Tibetan Plateau warming amplification in recent decades and future projections. *Journal of Climate*, *36*(17), 5775–5792. https://doi.org/10.1175/JCLI-D-22-0471.1
Hu, X., Li, Y., Yang, S., Deng, Y., & Cai, M. (2017). Process-based decomposition of the decadal climate difference between 2002–13 and 1984–95. *Journal of Climate*, *30*(12), 4373–4393. https://doi.org/10.1175/JCLI-D-15-0742.1
Huang, Y. (2022). ERA-interim reanalysis based radiative kernels [Dataset]. *Mendeley Data*. https://doi.org/10.17632/3drx8fmmz9.1
Liu, X., Cheng, Z., Yan, L., & Yin, Z.-Y. (2009). Elevation dependency of recent and future minimum surface air temperature trends in the Tibetan Plateau and its surroundings. *Global and Planetary Change*, *68*(3), 164–174. https://doi.org/10.1016/j.gloplacha.2009.03.017
Lu, J., & Cai, M. (2009). A new framework for isolating individual feedback processes in coupled general circulation climate models. Part I: Formulation. *Climate Dynamics*, *32*(6), 873–885. https://doi.org/10.1007/s00382-008-0425-3
O'Neill, B. C., Tebaldi, C., van Vuuren, D. P., Eyring, V., Friedlingstein, P., Hurtt, G., et al. (2016). The scenario model intercomparison project (ScenarioMIP) for CMIP6. *Geoscientific Model Development*, *9*(9), 3461–3482. https://doi.org/10.5194/gmd-9-3461-2016
Pendergrass, A. G. (2017). CAM5 radiative kernels [Dataset]. *UCAR/NCAR Earth System Grid*. https://doi.org/10.5065/D6F47MT6
Peng, X., Frauenfeld, O. W., Jin, H., Du, R., Qiao, L., Zhao, Y., et al. (2021). Assessment of temperature changes on the Tibetan Plateau during 1980–2018. *Earth and Space Science*, *8*(4), e2020EA001609. https://doi.org/10.1029/2020EA001609
Peng, Y., Duan, A., Hu, W., Tang, B., Li, X., & Yang, X. (2022). Observational constraint on the future projection of temperature in winter over the Tibetan Plateau in CMIP6 models. *Environmental Research Letters*, *17*(3), 034023. https://doi.org/10.1088/1748-9326/ac541c
Pithan, F., & Mauritsen, T. (2014). Arctic amplification dominated by temperature feedbacks in contemporary climate models. *Nature Geoscience*, *7*(3), 181–184. https://doi.org/10.1038/ngeo2071
Qiu, J. (2008). China: The third pole. *Nature*, *454*(7203), 393–396. https://doi.org/10.1038/454393a
Rangwala, I., Miller, J. R., & Xu, M. (2009). Warming in the Tibetan Plateau: Possible influences of the changes in surface water vapor. *Geophysical Research Letters*, *36*(6), L06703. https://doi.org/10.1029/2009GL037245
Refsgaard, J. C., van der Sluijs, J. P., Brown, J., & van der Keur, P. (2006). A framework for dealing with uncertainty due to model structure error. *Advances in Water Resources*, *29*(11), 1586–1597. https://doi.org/10.1016/j.advwatres.2005.11.013
Sharmila, S., Joseph, S., Sahai, A. K., Abhilash, S., & Chattopadhyay, R. (2015). Future projection of Indian summer monsoon variability under climate change scenario: An assessment from CMIP5 climate models. *Global and Planetary Change*, *124*, 62–78. https://doi.org/10.1016/j.gloplacha.2014.11.004
Shen, Z., Zhou, W., Li, J., & Chan, J. C. L. (2023). A frequent ice-free Arctic is likely to occur before the mid-21st century. *npj Climate and Atmospheric Science*, *6*(1), 103. https://doi.org/10.1038/s41612-023-00431-1
Shiogama, H., Watanabe, M., Kim, H., & Hirota, N. (2022). Emergent constraints on future precipitation changes. *Nature*, *602*(7898), 612–616. https://doi.org/10.1038/s41586-021-04310-8
Smith, C. (2019). HadGEM3-GA7.1 radiative kernels [Dataset]. *Zenodo*. https://doi.org/10.5281/zenodo.3594673
Soden, B. J., Held, I. M., Colman, R., Shell, K. M., Kiehl, J. T., & Shields, C. A. (2008). Quantifying climate feedbacks using radiative kernels. *Journal of Climate*, *21*(14), 3504–3520. https://doi.org/10.1175/2007JCLI2110.1
Su, F., Duan, X., Chen, D., Hao, Z., & Cuo, L. (2013). Evaluation of the global climate models in the CMIP5 over the Tibetan Plateau. *Journal of Climate*, *26*(10), 3187–3208. https://doi.org/10.1175/JCLI-D-12-00321.1
Su, J., Duan, A., & Xu, H. (2017). Quantitative analysis of surface warming amplification over the Tibetan Plateau after the late 1990s using surface energy balance equation. *Atmospheric Science Letters*, *18*(3), 112–117. https://doi.org/10.1002/asl.732
Tian, D., Guo, Y., & Dong, W. (2015). Future changes and uncertainties in temperature and precipitation over China based on CMIP5 models. *Advances in Atmospheric Sciences*, *32*(4), 487–496. https://doi.org/10.1007/s00376-014-4102-7
Wang, Q., Fan, X., & Wang, M. (2014). Recent warming amplification over high elevation regions across the globe. *Climate Dynamics*, *43*(1–2), 87–101. https://doi.org/10.1007/s00382-013-1889-3
Wu, J., & Gao, X. (2013). A gridded daily observation dataset over China region and comparison with the other datasets. *Chinese Journal of Geophysics*, *56*, 1102–1111. https://doi.org/10.6038/CJG20130406
Wu, J., Gao, X., Giorgi, F., & Chen, D. (2017). Changes of effective temperature and cold/hot days in late decades over China based on a high resolution gridded observation dataset. *International Journal of Climatology*, *37*(S1), 788–800. https://doi.org/10.1002/joc.5038
Wu, Y., Yang, S., Hu, X., & Wei, W. (2020). Process-based attribution of long-term surface warming over the Tibetan Plateau. *International Journal of Climatology*, *40*(15), 6410–6422. https://doi.org/10.1002/joc.6589
Yang, K., He, J., Tang, W., Lu, H., Qin, J., Chen, Y., & Li, X. (2019). China meteorological forcing dataset (1979-2018) [Dataset]. *National Tibetan Plateau/Third Pole Environment Data Center*. https://doi.org/10.11888/AtmosphericPhysics.tpe.249369.file
Yang, M., Wang, X., Pang, G., Wang, G., & Liu, Z. (2019). The Tibetan Plateau cryosphere: Observations and model simulations for current status and recent changes. *Earth-Science Reviews*, *190*, 353–369. https://doi.org/10.1016/j.earscirev.2018.12.018
Yao, T., Xue, Y., Chen, D., Chen, F., Thompson, L., Cui, P., et al. (2019). Recent third pole's rapid warming accompanies cryospheric melt and water cycle intensification and interactions between monsoon and environment: Multidisciplinary approach with observation, modeling, and analysis. *Bulletin of the American Meteorological Society*, *100*(3), 423–444. https://doi.org/10.1175/bams-d-17-0057.1
You, Q., Cai, Z., Pepin, N., Chen, D., Ahrens, B., Jiang, Z., et al. (2021). Warming amplification over the Arctic pole and third pole: Trends, mechanisms and consequences. *Earth-Science Reviews*, *217*, 103625. https://doi.org/10.1016/j.earscirev.2021.103625
You, Q., Cai, Z., Wu, F., Jiang, Z., Pepin, N., & Shen, S. S. P. (2021). Temperature dataset of CMIP6 models over China: Evaluation, trend and uncertainty. *Climate Dynamics*, *57*(1–2), 17–35. https://doi.org/10.1007/s00382-021-05691-2
You, Q., Jiang, Z., Moore, G., Bao, Y., Kong, L., & Kang, S. (2017). Revisiting the relationship between observed warming and surface pressure in the Tibetan Plateau. *Journal of Climate*, *30*(5), 1721–1737. https://doi.org/10.1175/JCLI-D-15-0834.1
You, Q., Wu, F., Shen, L., Pepin, N., Jiang, Z., & Kang, S. (2020). Tibetan Plateau amplification of climate extremes under global warming of 1.5° C, 2°C and 3°C. *Global and Planetary Change*, *192*, 103261. https://doi.org/10.1016/j.gloplacha.2020.103261

Yu, Y., Mao, J., Wullschleger, S. D., Chen, A., Shi, X., Wang, Y., et al. (2022). Machine learning-based observation-constrained projections reveal elevated global socioeconomic risks from wildfire. *Nature Communications*, *13*(1), 1250. https://doi.org/10.1038/s41467-022-28853-0

Zhang, J., You, Q., Wu, F., Cai, Z., & Pepin, N. (2022). The warming of the Tibetan Plateau in response to transient and stabilized 2.0°C/1.5°C global warming targets. *Advances in Atmospheric Sciences*, *39*(7), 1198–1206. https://doi.org/10.1007/s00376-022-1299-8

Zhang, R., Wang, H., Fu, Q., & Rasch, P. J. (2020). Assessing global and local radiative feedbacks based on AGCM simulations for 1980–2014/2017. *Geophysical Research Letters*, *47*(12), e2020GL088063. https://doi.org/10.1029/2020GL088063

Zhou, M., Yu, Z., Gu, H., Ju, Q., Gao, Y., Wen, L., et al. (2022). Evaluation and projections of surface air temperature over the Tibetan Plateau from CMIP6 and CMIP5: Warming trend and uncertainty. *Climate Dynamics*, *60*(11–12), 3863–3883. https://doi.org/10.1007/s00382-022-06518-4

Zhou, T., & Zhang, W. (2021). Anthropogenic warming of Tibetan Plateau and constrained future projection. *Environmental Research Letters*, *16*(4), 044039. https://doi.org/10.1088/1748-9326/abede8

References From the Supporting Information

Brunner, L., Pendergrass, A. G., Lehner, F., Merrifield, A. L., Lorenz, R., & Knutti, R. (2020). Reduced global warming from CMIP6 projections when weighting models by performance and independence. *Earth System Dynamics*, *11*(4), 995–1012. https://doi.org/10.5194/esd-11-995-2020

Hersbach, H. (2000). Decomposition of the continuous ranked probability score for ensemble prediction systems. *Weather and Forecasting*, *15*(5), 559–570. https://doi.org/10.1175/1520-0434(2000)015<0559:DOTCRP>2.0.CO;2

Huang, Y., Xia, Y., & Tan, X. (2017). On the pattern of CO_2 radiative forcing and poleward energy transport. *Journal of Geophysical Research: Atmospheres*, *122*(20), 10578–10593. https://doi.org/10.1002/2017JD027221

Kramer, R. J., Matus, A. V., Soden, B. J., & L'Ecuyer, T. S. (2019). Observation-based radiative kernels from CloudSat/CALIPSO. *Journal of Geophysical Research: Atmospheres*, *124*(10), 5431–5444. https://doi.org/10.1029/2018JD029021

Pendergrass, A. G., Conley, A., & Vitt, F. M. (2018). Surface and top-of-atmosphere radiative feedback kernels for CESM-CAM5. *Earth System Science Data*, *10*(1), 317–324. https://doi.org/10.5194/essd-10-317-2018

Shell, K. M., Kiehl, J. T., & Shields, C. A. (2008). Using the radiative kernel technique to calculate climate feedbacks in NCAR's Community Atmospheric Model. *Journal of Climate*, *21*(10), 2269–2282. https://doi.org/10.1175/2007JCLI2044.1

Smith, C. J., Kramer, R. J., & Sima, A. (2020). The HadGEM3-GA7.1 radiative kernel: The importance of a well-resolved stratosphere. *Earth System Science Data*, *12*(3), 2157–2168. https://doi.org/10.5194/essd-12-2157-2020